High Resolution fMRI Reveals Distinct Forms of Associative Novelty in the Medial Temporal Lobe

Presented By: Christine Manthuruthil

In partial fulfillment of the requirements for graduation with the Dean's Scholars Honor's Degree in Biology

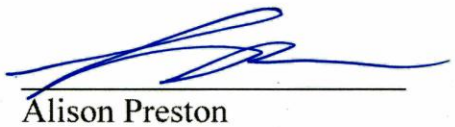

Alison Preston
Supervising Professor

5/10/2012
Date

Abstract

Both Alzheimer's Disease and Parkinson's Disease involve alterations to the structure of the medial temporal lobe (MTL). Varying patterns of neuronal connectivity, however, suggest that not only does the MTL support learning and memory, but that its subregions play distinct roles in these processes as well. The exact nature of these contributions remains an area of active investigation. Examinations of associative novelty may offer an important tool for characterizing the processes carried out by different subregions. Associative novelty can be further broken down into associative novelty per se, which are simply novel stimulus configurations, and associative mismatch novelty, which are novel stimulus configurations that violate existing expectations. In this study, we used high resolution fMRI to characterize different associative novelty signals across the MTL; specifically, we were interested in whether there was a dissociation of associative novelty signal types between MTL subregions, or instead, a functional specialization for associative novelty signal types distributed across these subregions. Establishing subregional function could help elucidate the spectrum of cognitive deficits manifest in both Parkinson's and Alzheimer's patients

Introduction

Of the 5.1 million Americans that have Alzheimer's Disease and the nearly half a million that suffer from Parkinson's Disease, alterations to the medial temporal lobe (MTL) of the brain are present in nearly all cases [1-2]. MTL atrophy serves as a hallmark indicator of both diseases [3-4]. The correlation between these diseases' differential action on the MTL and their associated spectrums of potential cognitive impairment remains an area of active investigation. The MTL—inclusive of the hippocampal formation (encompassing the CA1, CA2, and CA3 subfields, the dentate gyrus, and subiculum) and the surrounding entorhinal, perirhinal, and parahippocample cortices (ERC, PRC, and PHC, respectively)—has been well implicated in learning and memory [5]. Damage to the MTL produces deficits in *declarative memory*, long-term memory for specific facts (*semantic memory*) and specific events (*episodic memory*) [6]. Varying patterns of neuronal connectivity within the MTL further suggest that its subregions play distinct roles in these processes [5-6]. Establishing subregional function, then, could shed light on the etiology of the particular symptoms that manifest within a particular Parkinson's or Alzheimer's patient.

The diverse cytoarchitecture of the MTL consists of numerous neuronal inputs and outputs, both within the MTL and outside of it, which support assorted features of declarative memory. For instance, PRC receives inputs from visual association areas integral to visual object processing while PHC receives inputs from visual association areas more concerned with visuospatial processing. PHC and PRC in turn output to discrete areas of the ERC, effectively preserving the segregation of visual object and visuospatial information [7-8]. PRC neurons further exhibit familiarity-based novelty response patterns to multiple stimulus exposures such that maximal responses occur during the first exposure and are sharply attenuated with subsequent encounters [6]. The ERC, on the other hand, provides inputs to the dentate gyrus,

CA1, and CA3 subfields of the hippocampus [6]. The extensive recurrent circuitry within CA3 might underlie *pattern completion* processes that reactivate stored memory representations from partial or degraded inputs, and the combination of ERC input with this extensive recurrent circuitry corroborates with a role in binding the disparate activation patterns elicited by an event into an integrated memory representation [9]. CA1 lacks this multiplicity of associational connections, but its convergent inputs from CA3 and ERC indicate a potential function as a novelty detector through the comparison of current events (i.e. sensory information transmitted by ERC) with stored memory representation (i.e. pattern completion processes mediated by CA3) [10].

Novelty responses, overall, are ideal tools for dissecting subregional function in the MTL [11]. While most investigations of MTL contributions to learning and memory center on individual item memory, MTL-based episodic memory—deficits in which produce the most striking symptoms of Alzheimer's Disease—does not depend on memory representation of individual stimuli. Episodic memory is inherently associative: it distills the relationships between the particular people, places, objects, and actions that comprise an even into a coherent, composite memory representation. Because we are interested in the deficits in memory introduced by Alzheimer's and Parkinson's Diseases, and the MTL is a primary site of action for both diseases, our study will focus on associative novelty, a form of episodic memory that deals with new versus old stimulus configurations. There are two types: associative novelty per se, which are simply novel stimulus configurations, and associative mismatch novelty, which are novel stimulus configurations that violate existing expectations. For example, seeing a man walking his dog might activate associative novelty per se; on the other hand, seeing a woman walking the same dog at a later date might activate associative mismatch novelty.

The within-episode binding carried out in CA3 could potentially suffice for associative novelty per se, but associative mismatch novelty uniquely necessitates reactivation and comparison with stored memory representations [12]. Two computations are at work here: CA3 pattern completion to retrieve stored memory representations and CA1 novelty detection to identify for unanticipated mismatches between these stored memory representations and incoming stimulus configurations. We hypothesize, based on the recurrent circuitry in CA3 and the combinatorial input of CA3 and ERC to CA1, that associative mismatch novelty will preferentially activate CA1 novelty detection mechanisms to support the recognition of violated expectations producing a dissociation of associative novelty signal types between the CA1 and CA3 subfields.

Recent work offers evidences that the two forms of associative novelty detection could also instigate separate learning processes. Associative novelty per se may sustain the aforementioned integration of disparate activation patterns associated with an event into a cohesive memory representation [13]. Associative mismatch signals, conversely, may trigger the integration of information from discrete experiences, binding together elements across individual events [14]. This integrative encoding flexibly generalizes information across memory representations to identify non-explicit relationships between multiple events. Memory-based predictions could thereby serve as the foundation for inferential processes (harking back to our earlier example, the mismatch between the current event of the woman walking the dog with the stored memory representation of the man walking the dog would prompt the formation of an integrated man-dog-woman representation of the two overlapping events).

Midbrain regions such as the ventral tegmental area (VTA) and substantia nigra (SN) may serve associative novelty—more expressly, associative mismatch novelty—as well. MTL

regions enhance learning in response to and provide feedback through CA1 to dopamine neurons in VTA [15]. Neuroimaging studies have also shown indications of midbrain-MTL interactions during the presentation of novel stimuli [15]. Midbrain neurons maximally respond to current events that violate pre-existing expectations. This prediction error signal, while typically associated with reward processes, could output to MTL regions and alter existing computations to enhance novelty detection and integrative encoding.

To investigate whether these two associative novelty process dissociate anatomically across the MTL, participants learned a series of overlapping (pairs that share a member in common) and non-overlapping object pairs (pairs that have no common members) designed to elicit associative mismatch novelty and associative novelty responses, respectively, while undergoing high-resolution functional magnetic resonance imaging (fMRI). fMRI plays a crucial role in unifying computational, animal, and human approaches to the investigation of MTL function. Standard-resolution fMRI, however, lacks the spatial resolution necessary to probe the functional heterogeneity within MTL suggested by emerging rodent data and theoretical models. Since the initial application of high-resolution fMRI to the MTL, however, researchers have been able to use underlying cytoarchitectural landmarks to partition the MTL into its hippocampal subfields and surrounding cortices [16-17]. High-resolution fMRI, with a spatial resolution less than or equal to 2 x 2 mm (relative to standard resolution fMRI data with a resolution closer to 4x4 mm), along with advances in MR hardware and data analysis, have allowed to the localization of activation to individual subfields. Using high-resolution fMRI , then, we can address the differential participation of MTL subfields in various aspects of declarative memory, in general, and associative novelty, specifically [18]. Consequently, our study informs the

ongoing interrogation and refinement of theoretical declarative memory circuits that have been so far based largely off emergent rodent data.

Material and Methods

Participants: Twenty-nine healthy, English-speaking individuals (18 females, ages 18-27, mean age = 21) participated in the experiment after giving informed consent in accordance with a protocol approved by the Institutional Review Boards of Stanford University and The University of Texas at Austin. Participants received $20/h for their involvement. Data from seven participants were excluded from analysis due to excessive head motion (4 participants), anatomical anomalies (1 participant), equipment malfunction resulting in incorrect timing (1 participant), and non-compliance (1 participant). Consequently, data from twenty-two participants (15 females, mean age = 21) were included in the fMRI analyses.

Materials: Stimuli consisted of 240 color images of common objects arranged into 96 overlapping object pairs (48 AB, 48 BC) and 48 unique, nonoverlapping objects pairs (XY) (Fig 1A). Overlapping AB and BC pairs were composed such that two objects (A and C) shared an association with a third, overlapping member (B). XY pairs were composed of two unique objects that shared no associations with other pairings. Participants were assigned to one of six randomization groups to counterbalance the presentation of stimuli across pair types and the order of presentation.

Procedure: The task, modeled after the associative inference paradigm consisted of two phases: (1) an encoding phase during which participants intentionally learned associations between

object pairs (AB, BC, XY), and (2) a test phase during which participants were tested on trained (AB, BC, XY) as well as untrained inferential (AC) associations. High resolution functional magnetic resonance imaging (fMRI) data were collected during the encoding phase. Participants were instructed that they would be tested on directly learned associations (AB, BC, XY) as well as indirectly related inferential (AC) associations, and were given the opportunity to practice both the encoding and test phases of the experiment prior to scanning.

For each encoding run, participants learned 8 associations of each type (AB, BC, XY) presented in a pseudo-random rapid event-related design. All object pairs were presented three times, but within each ABC triad, the first presentation of a BC pair always interleaved between the first and second presentations of its corresponding AB pair (Fig 1B). The threefold presentation of individual trials allowed for the identification of regions uniquely involved with associative mismatch novelty or associative novelty per se. This relies on a key feature of overlapping pairs relative to non-overlapping pairs. Non-overlapping XY pairs do not relay novel content during their second and third presentations. Instead, they simply become more familiar with each presentation. The shared B member of overlapping AB and BC pairs, on the other hand, creates a unique set of circumstances for the members of each triad. While the first presentation of AB pairs is analogous to the first presentation of XY pairs, it sets up an expectation (AB) that is violated by the first presentation of its corresponding BC pair. Subsequent AB presentations in this way generate novel "mismatches" with BC pairs absent during the first AB presentations.

Participants were advised to make use of stories linking the members of a pair to improve performance, then asked to rate the quality of their story during pair presentation using a 4 point (1=no story, 2=poor story, 3=good story, 4=best story). These assessments acted to secure

participants' attention during the encoding phase and were not considered in the fMRI data analysis [19]. Each task trial consisted of a 3.5 second stimulus presentation followed by a .5 second fixation period. Trial onsets were jittered with a variable number (0, 2, 4, 6, or 8) of odd/even digit baseline trials (Stark and Squire, 2001) using a sequence optimization program (Dale, 1999) to allow for event-related analyses. Baseline trials consisted of a 2 second presentation of a single digit between 1 and 8 during which participants indicated whether the digit was odd or even.

After six encoding runs, participants were tested outside the scanner on directly learned associations (AB, BC, XY) and inferential (AC) associations using a 2-alternative forced-choice paradigm. In the course of each self-paced test trial, a single cue object (e.g. an A object) was presented on the top of the screen and two object choices present on the bottom of the screen (e.g. two B objects) (Fig 1D). Participants were required to make a decision indicating which of the two choice objects were associated with the cue. For inferential AC associations, participants were instructed that the association between the cue (A) and the correct choice (C) was indirectly mediated through a third object that shared an association with both the cue and the correct choice during encoding (B). Foils for these trials were other familiar C objects studied during the encoding phase that did not share a common association with the cue.

Individual inferential AC trials were presented before the corresponding AB and BC associations to avoid learning associations between A and C objects during test. Of note, for both trained and inferential associations, foils were all familiar items that had been encountered in the context of another object distinct from the cue. Correct responses, therefore, could not rely on familiarity-based judgments regarding the choice object, but instead required the retrieval of learned associations.

fMRI data acquisition: Imaging data were collected on a 3.0 T GE Signa whole-body MRI system (GE Medical Systems, Milwaukee, WI, USA) with an 8-channel head coil array High-resolution, T2-weighted, flow-compensated spin-echo structural images (TR = 3s, TE = 68 ms, 0.43 x 0.43 inplane resolution) were acquired in advance of functional scanning using 20 3-mm thick slices perpendicular to the main axis of the hippocampus to enable visualization of hippocampal subfields and MTL cortical subregions. A high-resolution T2*-sensitive gradient echo spiral in/out pulse sequence (Glover & Law, 2001) was used to gather functional images with the same slice locations as the structural images (TR= 4s, TE = 34 ms, flip angle = 80°, FOV = 22 cm, 1.7 x 1.7 x 3.0 mm resolution). A high-order shimming procedure based on spiral acquisitions was employed to reduce B_0 heterogeneity prior to functional scanning. Importantly, spiral in/out methods increase SNR and BOLD contrast-to-noise ration in uniform brain regions while diminishing signal loss in regions jeopardized by susceptibility induced field gradients (SFG) (Glover & Law, 2001), including the anterior MTL. Spiral in/out methods result in less signal dropout and greater task-related activation in MTL (Preston, Thomason, Oschsner, Cooper, & Glover, 2004) relative to other imaging techniques (Glover & Lai, 1998), enabling the examination of structure previously inaccessible due to SFG.

648 total volumes were acquired for each participant. In order to obtain a field map for the correction of magnetic filed heterogeneity, the echo time of the first time frame of the functional timeseries was 2 ms longer than all subsequent frames. The map for each slice was calculated from the phase of the first two time frames and applied as a first order correction during reconstruction of the functional images thereby minimizing blurring and geometric distortion on a per-slice bases. Correction for off-resonance due to breathing was applied on a

per-time-frame basis as well via phase navigation (Pfeuffer, Van de Moortele, Ugurbil, Hu, & Glover, 2002). This initial volume, in addition to the following two volumes of each scan (a total of 12s), was then discarded to allow for T1 stabilization.

fMRI data analysis: (to be written in lab): Data were preprocessed and analyzed using SPM5 (Wellcome Department of Cognitive Neurology, London, UK) and custom MATLAB (MathWorks, MA) routines. Differences in functional image slice acquisition times were corrected for by interpolating the voxel time series using sinc interpolation and resampling the time series with the center slice as a reference point. Next, to account for motion, these images were realigned to the first volume of the time series. The realigned data were filtered with a 128s high-pass filter and converted to percent signal. Structural images were coregistered to the mean functional image computed during realignment.

First-level, individual analyses proceeded under the assumptions of the general linear model (Worsley & Friston, 1995). Successive study runs were appended and analyzed collectively for each subject as a function of nine regressors, along with a temporal derivative to account for differences in latency of the peak response elicited by stimulus presentations. These regressors expressed the range of task conditions: the first, second, or third repetition of AB, BC, or XY stimulus pairs.

Second-level group analyses followed landmark-based normalization in ANTS to a model template (1.5 x 1.5 x 1.5 mm resolution) created from a composite of participants' structural data centered at the anterior commissure [20]. A hand-drawn MTL mask—inclusive of bilateral hippocampus and bilateral entorhinal (ERC), perirhinal (PRC), and parahippocampal (PHC) cortices—guided the generation of linear and non-linear transformation matrices that were then applied to first-level contrasts and beta images. Compared with normalization to a

standard template, this procedure enabled the detection of activation signals common to all subjects while simultaneously preserving the high spatial precision essential to classifying these signals within specific subfields.

For all comparisons, group-level statistical maps were first created using an uncorrected voxel-wise threshold of $p < .025$. A small-volume correction was employed to establish a cluster-level corrected threshold of $p < .05$ to correct for multiple comparisons. Small-volume correction was determined through Monte Carlo simulations run via the AlphaSim tool in AFNI that take into account the size and shape of each region in addition to the height threshold p-value and smoothness of actual data. Simulations were performed for MTL and SN/VTA bilaterally. Cluster sizes that occurred with probability less than .05 across 5000 simulations were considered significant. This yielded a minimum cluster size of 65 voxels for MTL, and 50 voxels for SN/VTA. The subsequent group-level results were then anatomically masked to inspect condition-specific responses in MTL subregions and SN/VTA.

The two contrasts used to isolate candidate regions for associative novelty per se and associative mismatch novelty relied on differential responses to the establishment of an expectation by the first presentation of an AB pair and the violation of that expectation by its corresponding BC pair. Specifically, we parsed AB and XY repetitions for activation patterns related to associative novelty per se and associative mismatch novelty. As stated above, the intervening BC pair between the first and second AB repetitions causes AB and XY pairs to dissociate: XY pairs reiterate progressively less novel information and AB pairs continue to provoke mismatches with BC pairs. The first presentations of AB and XY pairs, however, are uniquely analogous in that both deliver novel information that does not violate prior expectations. This correspondence ideally positions AB and XY repetitions to resolve

comparisons between associative mismatch novelty and associative novelty per se activations patterns. BC pairs were excluded here due to their lack of cognate with XY pairs: upon their first presentation, BC pairs already violate the expectations established by a preceding AB pair.

Associative novelty per se activation patterns *would not* recognize the mismatch between corresponding AB and BC pairs and instead encode AB and XY stimulus pairs as less novel with each presentation. Accordingly, the repetition suppression contrast that we performed to isolate candidate regions for associative novelty per se selected for decreasing activation between the first and third repetitions of AB and XY pairs [(AB1+XY3)>(AB3+XY3)]. Associative mismatch novelty processes *would* recognize that while latter presentations of XY pairs reiterated progressively less novel information, AB pairs provoked mismatches with BC pairs. Accordingly, the interaction contrast we performed to isolate candidate regions for associative mismatch novelty selected for increasing activation between the first and third AB repetitions relative to decreasing activation across the first and third XY repetitions [(AB3-AB1)>(XY3-XY1)]. Associative mismatch novelty signals thus underlay processes that coded the violation of expectations across repetitions of overlapping pairs relative to progressively less-novel non-overlapping pairs. Meanwhile, associative novelty per se signals underlay processes that treated both overlapping and non-overlapping pairs as progressively less novel with each presentation.

The masked group level repetition suppression and interaction contrasts yielded a set of candidate regions in MTL and SN/VTA. These functional regions of interest (fROIs) were defined by drawing comparisons between activation patterns elicited during the task conditions specified by the contrast. Using hand-drawn anatomical masks, we then separated fROIs by MTL and midbrain subregions. In hippocampus, these were (1)CA1, (2) CA2, CA3, and dentate

gyrus, (3) subiculum, (4) entorhinal cortex, (5) perirhinal cortex, and (6) parahippocampal cortex. In midbrain, these were SN/VTA.

To confirm whether activation patterns within these regions aligned with associative novelty per se or associative mismatch novelty, we next extracted beta values across AB and XY repetitions from the resultant batch of anatomically separated fROIs to define signal profiles for associative novelty per se and associative mismatch novelty. The difference in signal between the third and first repetitions of the two pair types was used to classify activation increases (positive numbers; third>first) and activation decreases (negative numbers; third<first). Activation plots subsequently do not represent the absolute value of the signal strength at any particular AB or XY condition (e.g. AB1, XY3), but rather, the difference in activation between the third and first repetitions of AB and XY pair types (e.g. AB3-AB1 and XY3-XY1). Patterns commensurate with associative novelty per se—due to their inattentiveness to mismatches between AB and BC pairs—would treat AB and XY pairs as similarly less novel with each presentation and demonstrate comparable signal decreases across AB and XY repetitions (AB3<AB1; XY3<XY1) (Fig 1C). In contrast, patterns commensurate with associative mismatch novelty—due to their attentiveness to mismatches between AB and BC pairs—would dissociate between AB and XY pairs and demonstrate signal increase across AB repetitions (AB3>AB1) and signal decrease across XY repetitions (XY3<XY1) (Fig 1C).

Results

Behavioral Results: All participants successfully acquired trained object associations (mean =7% correct, SD =4%; t22)=54.40, df=21, p = .001). Performance on inferential associations, was significantly above chance (mean =89% correct, SD =13%; t22) =14.30, df=21 p = .001).

Notably, inferential performance varied across a larger range (range 56-100%) than for trained associations (range 79-100%). Where trained performance was more consistently high across participants, inferential performance showed greater individual differences; these dissimilar spreads in trained and inferential performance led us to examine correlations between inferential performance and individual ROI activations. At test, mean median reaction times for trained associations (1636 ms, SD _391ms) was significantly faster than for inferential associations (2999 ms, SD _1325 ms; t22)=5.05, df=21, p = .001).

Associative Novelty Per Se in MTL: To identify regions that show the hypothesized associative novelty per se signal (i.e. signal decrease across AB and XY repetitions) we identified a set of candidate regions using the repetition suppression contrast [(AB1+XY1)>(AB3+XY3)] (Fig 2A).

In MTL, these fell within left hippocampus, right hippocampus, bilateral PRC, and bilateral PHC. The corresponding beta values demonstrated a non-significant difference in suppression effects between AB and XY repetitions for left hippocampus (t22)=-1.64, df=21, p=.12), right hippocampus (t22)=, df=21 p=.12), and bilateral PRC ((t22)=-1.24, df=21, p=.23,) consistent with associative novelty per se profiles (Fig 2B). These regions, regardless of the intervening BC pairs, processed both AB and XY pairs as similarly less novel with additional presentations. Bilateral PHC beta values, however, expressed a significant difference in suppression across AB and XY repetitions (t22)=-2.94, df=21, p=.007). While its activity decreased for both AB and XY repetitions, the decrease across AB repetitions was significantly smaller than the decrease across XY repetitions. This suggests a degree of mismatch sensitivity.

In midbrain, the candidate regions fell within VTA/SN. The corresponding beta values demonstrate a non-significant difference in suppression between AB and XY repetitions for

VTA/SN consistent with associative novelty per se profiles (t22)=-1.26, df=21, p=.22) (Fig 2C).

Associative Mismatch Novelty in MTL: To identify regions that show the hypothesized associative mismatch signal (i.e. signal increase across AB repetitions, signal decrease across XY repetitions) we identified a set of candidate regions using the interaction contrast [(AB3-AB1)>(XY3-XY1)] (Fig 3A).

In MTL, these fell within left hippocampus, left ERC, bilateral PRC, and bilateral PHC. The corresponding beta values demonstrated a significant difference between increasing signals across AB repetitions and decreasing signals across XY repetitions for left ERC (t22)=-3.45, df=21 p=.002) and bilateral PRC (t22)=-5.51, df=21, p<.001) consistent with associative mismatch profiles (Fig 3B). These regions recognized and encoded the violation of expectations triggered by intervening BC pairs across AB repetitions relative to successively less novel XY repetitions. Bilateral PHC beta values exhibited a significant difference in *suppression* effects across AB and XY repetitions (t22)=-4.48, df=21, p<.001) (Fig 3B). Like the functional ROI isolated from the suppression contrast, its activity decreased across both AB and XY pairs but to a significantly lesser extent for AB pairs. Again, this suggests a degree of mismatch sensitivity.

Left hippocampus, spanning all subfields, expressed the same significant difference between increasing signals across AB repetitions and decreasing signals across XY repetitions (t22)=-3.08, df=21, p=.005), though the increase in signal across AB repetitions was not significantly greater than zero (t22)=-1.17, df=21, p=.25) (Fig 3B). Because of our a priori hypothesis of associative novelty differentiation within hippocampus derived from *in vitro* neuroanatomical studies of CA1 and CA3 hippocampal subfields, however, we further separated the left hippocampal ROI by hippocampal subfield. Notably, the extensive associational

connections within CA3 suggests a role in pattern completion processes that support the reactivation of stored memory representations from partial or degraded inputs. This dense recurrent circuitry might also work in conjunction with inputs from lateral and medial ERC to facilitate the binding of multiple, disparate activation patterns of an event into an integrated memory representation. On the other hand, the few associational connections within CA1 combined with the convergence of inputs from CA3 and ERC suggests a role in novelty detection processes that compare current events with stored memory representations for any mismatches.

Associative novelty detection in hippocampus may thus rely on the retrieval of stored representations through pattern completion mechanism in CA3 and the detection of mismatches between incoming stimulus configurations and these stored representations through novelty detection mechanisms in CA1. While associative novelty per se would fail to recruit CA1 novelty detection and CA3 pattern completion across latter repetitions of non-overlapping XY pairs, associative mismatch novelty may selectively drive CA1 comparator mechanisms across latter repetitions of overlapping AB pairs. In fact, consistent with our expectations, after separating the left hippocampal fROI by subfield, only CA1 demonstrated an associative mismatch novelty signature ($t_{22}=-2.13$, $df=21$, $p=.05$).

In midbrain, the candidate regions fell within VTA/SN. The corresponding beta values demonstrated a significant difference between increasing signals across AB repetitions and decreasing signals across XY repetitions ($t_{22}=-3.42$, $df=21$, $p=.003$) consistent with associative mismatch novelty profiles (Fig 3C).

To assess behavioral relevance of the associative mismatch signal, we correlated AB activation increases in the regions that showed the mismatch signal to inferential AC

performance across subject. Bilateral PRC associative mismatch signals tracked individual differences in AC performance, where participants who demonstrated greater increases in signal across AB repetitions had superior performance on inferential AC trials requiring the binding of information across episodes. (r=.52, p=.01, Fig. 4).

Discussion

Alzheimer's Disease and Parkinson's Disease act on MTL structures to generate patient-specific arrays of episodic memory deficits. Episodic memory is inherently associative insofar as events are aggregates of related people, places, objects, and actions. What's more, a subregion's novelty responses to a given change in sensory inputs (e.g. associative novelty) provide evidence that the subregion supports the relevant representations (i.e. associations) {ref}. Associative novelty, therefore, provides a key window into different subregion contributions to episodic memory. Our results revealed a distribution of associative novelty per se and associative novelty mismatch signals—sometimes functionally dissociated, sometimes anatomically dissociated—across MTL and midbrain subregions. In MTL, associative novelty per se signals fell within bilateral hippocampus, bilateral PRC, and bilateral PHC and associative mismatch novelty per se signals fell within left ERC, bilateral PRC, and left hippocampus. In midbrain, associative novelty per se and associative mismatch novelty signals both fell within VTA/SN. These findings collectively suggest that overlapping sets of MTL subregions sustain associative novelty per se and associative mismatch novelty. Alzheimer's Disease and Parkinson's Disease, therefore, can act at different combinations of MTL subregions to precipitate a particular deficit in episodic memory (e.g. deficits in associative novelty per se and associative mismatch novelty

could proceed from damage limited to bilateral PRC or from damage to both bilateral PHC and left ERC, etc.).

Our MTL findings seem at first to indicate a functional dissociation between associative novelty signal types, but further elaboration sheds light on a more complex picture. Foremost, due to a priori investigations of the distinct patterns of connectivity within the CA1 and CA3 subfields, we further separated the associative mismatch novelty signal in left hippocampus into its component subfields. The combination of CA3 (pattern completion) and ERC (incoming sensory information) output to CA1 attests to a novelty detector capable of distinguishing mismatches between stored memory representations with current events [9-10]. Due to the role of such a comparator in facilitating associative mismatch novelty processes, we hypothesized that CA1 would be preferentially stimulated over CA3 by associative mismatch novelty. Importantly, such localization of activation signals to individual hippocampal subfields could only occur because of our use of high-resolution fMRI; standard resolution fMRI would result in voxels too large to isolate activation signals within subfields. Our initial findings seemed to dispute the expected differentiation of associative novelty signals between CA1 and CA3, with both the bilateral hippocampal associative novelty per se signal and the left hippocampal associative mismatch novelty signal spanning across hippocampal subfields. Our additional analysis, however, revealed that only CA1 displayed a significant associative mismatch novelty signal. This CA1-restricted associative mismatch novelty signal coheres with the characteristic cytoarchitecture of the subfield.

Turning to our cortical findings, we find that the PHC signals isolated using both the repetition suppression [(AB1+XY3)>(AB3+XY3)] and interaction [(AB3-AB1)>(XY3-XY1)] contrasts exhibited a significant difference in suppression effects. That is, activation in response

to non-overlapping XY pairs diminished significantly more across repetitions than activation in response to AB pairs that shared their B member with a corresponding BC pair. This significant difference in signal decrease between AB and XY pairs might result from a degree of mismatch sensitivity in PHC.

We note next that both associative novelty per se and associative mismatch novelty signals are present in PRC. Standard-resolution fMRI would likely merge together discrepant associative novelty signals in close enough proximity to exist within the same subregion. High-res fMRI, on the other hand, possesses the resolution necessary to discretely identify the two patterns of activation. In addition, the PRC associative mismatch novelty signal engages in a larger debate surrounding PRC function. While PRC has previously been categorized as a processor of item novelty, recent literature indicates that it might mirror CA1 and assist associative mismatch novelty processes [21]. Significantly, this mismatch signal cannot proceed from stimulus-class bias. If item novelty alone incited PRC, we would expect to see a greater decrease in activity evoked by AB pairs as opposed to XY pairs across repetitions. The B member of an AB pair would appear again in BC presentations, rendering B the most familiar object and AB pairs more familiar than XY pairs via computations of item novelty. Rather, the PRC associative mismatch novelty signal could reflect one of two processes. First, it could be a downstream effect of CA1 associative mismatch novelty output. Alternatively, PRC could directly compute associative mismatch novelty. Given the larger role of PRC in encoding item information, it remains to be seen whether this associative mismatch signal would generalize to non-object classes of stimuli. ERC showed an associative mismatch novelty signal akin to that in PRC but no associative novelty per se signal.

Our midbrain findings of associative novelty per se and associative mismatch signals in the SN/VTA bring to bear on the theorized hippocampal-VTA loop. Here, hippocampal associative novelty per se signals are thought to improve learning by enhancing VTA dopaminergic output that spark the encoding of new events [15]. The appearance of both associative novelty per se and associative mismatch novelty signals in SN/VTA indicate that associative mismatch novelty may partake in a similar circuit. In this case, associative mismatch novelty signals would serve as a "prediction error" signal that then up-regulates VTA dopamine release to trigger the integrative encoding of information across events that permits inferential judgments [21]. Unfortunately, the directionality of the theorized hippocampal-VTA loop remains to be determined. Current fMRI techniques lack the temporal resolution to conclude whether hippocampal output incites VTA activity or vice versa. It remains to be seen whether Alzheimer's and Parkinson's patients difficulties with episodic memory emerge due primarily to degeneration in the MTL, or, otherwise, due to breakage in this hippocampal-VTA loop. It is possible that, without dopamine signals from VTA, hippocampus fails to encode new content.

Taking into account prior indications that associative novelty per se and associative mismatch novelty provoke distinct learning processes, we had reason to search our set associative novelty signals for behavioral correlations. Associative novelty per se, given its hypothesized role in within-episode binding, ought to track performance on directly learned (AB, BC, and XY) predicated on explicit relationships confined to a particular pair [13]. Likewise, associative mismatch novelty, given its hypothesized role in integrative encoding, ought to track performance on indirectly learned (AC) pairs predicated on the flexible generalization of information across AB and BC pairs [14]. Due to consistently high participant performance on directly learned pairs, we were unable to link associative novelty per se with participant memory

for direct pairs at test. Performance on indirectly learned pairs, on the other hand, varied to a far greater degree across participants, and we were able to link associative mismatch novelty activity in PRC with participant memory for indirect pairs at test. This link to behavior, furthermore, could have potential diagnostic applications in Alzheimer's Disease and Parkinson's Disease: deficits in a patient's capacity to carry out associative mismatch novelty processes could serve as indicators of diminished function in PRC.

This study of associative novelty signal types, therefore, suggests a combination of functional and anatomical dissociation of associative novelty signal types across MTL and midbrain subregions. This implies that Alzheimer's Disease and Parkinson's Disease can act on multiple regions to induce a particular impairment with regards to episodic memory. Our midbrain findings, along with prior formulations of the hippocampal-VTA loop, challenge earlier intuitions that damages to MTL subregions were primary effectors of episodic memory defects. Finally, the correlation between the PRC associative mismatch novelty signal and AC performance demonstrates a like to behavior that could have important diagnostic applications. On the whole, these results provide evidence that episodic memory is maintained by associative novelty signals spanning midbrain and the MTL whose functional contributions often align with the underlying cytoarchitecture. This complex circuitry, moreover, reveals numerous potential sites through which Alzheimer's and Parkinson's induced degeneration can debilitate episodic memory. Different degrees of damage to variable combinations of MTL and midbrain subregions could well ground the spectrum of cognitive deficits that materialize throughout the population of Alzheimer's and Parkinson's patients.

Figures

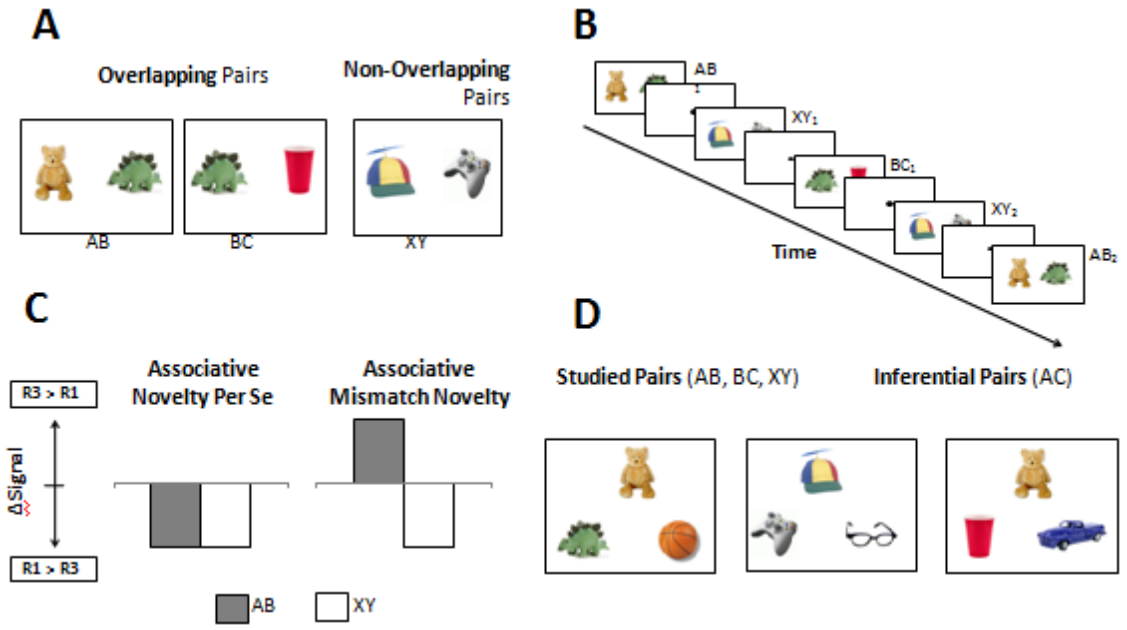

Figure 1. Task design and analysis strategy. A-C. Encoding phase. A. Participants studied overlapping (AB, BC) and non-overlapping (XY) object pairs while undergoing high-resolution functional MRI. B. Each object pair was presented three times. Trials were randomly intermixed with a restriction that overlapping pairs are presented in an interleaved manner (AB, BC, AB …). C. Hypothesized encoding activation signatures of associative novelty per se and associative mismatch novelty. Regions coding for associative novelty per se are expected to show decreasing activation across repeated presentations of both overlapping (AB) and non-overlapping (XY) object pairs. Regions coding for associative mismatch novelty are expected to show decreases across repeated presentations of non-overlapping (XY) pairs, but increasing activation across overlapping (AB) pairs. D. Unscanned test. Participants were tested on directly learned (AB, BC, XY) as well as inferential (AC) associations using a two alternative forced-choice test.

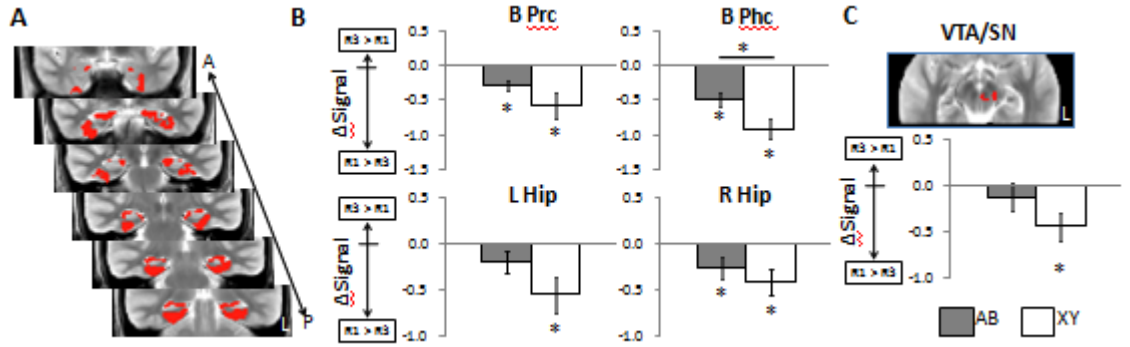

Figure 2. Associative novelty per se. A. Candidate regions: medial temporal lobe regions showing overall decreases of activation across repetitions overlaid on the group template. B. Changes in parameter estimates across encoding repetitions of overlapping (AB, gray bars) and non-overlapping (XY, white bars) pairs. Negative values represent activation decreases. Star above individual bars designates significant decreases at $p<0.05$, starred bar designates significant condition*repetition interaction at $p<0.05$. C. Location and activation pattern in a VTA/SN region that showed overall activation decreases across repetitions.

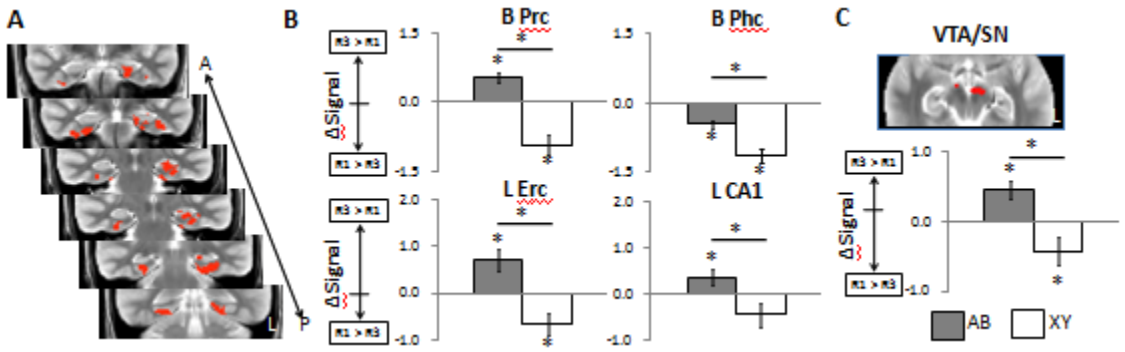

Figure 3. Associative mismatch novelty. A. Candidate regions: medial temporal regions showing condition*repetition interaction overlaid on the group template. B. Changes in parameter estimates across encoding repetitions of overlapping (AB, gray bars) and non-overlapping (XY, white bars) pairs. Negative values represent activation decreases, positive values represent activation increases. Star above individual bars designates significant decrease/increases at $p<0.05$, starred bar designates significant condition*repetition interaction at $p<0.05$. C. Location and activation pattern in a VTA/SN region that showed condition*repetition interaction.

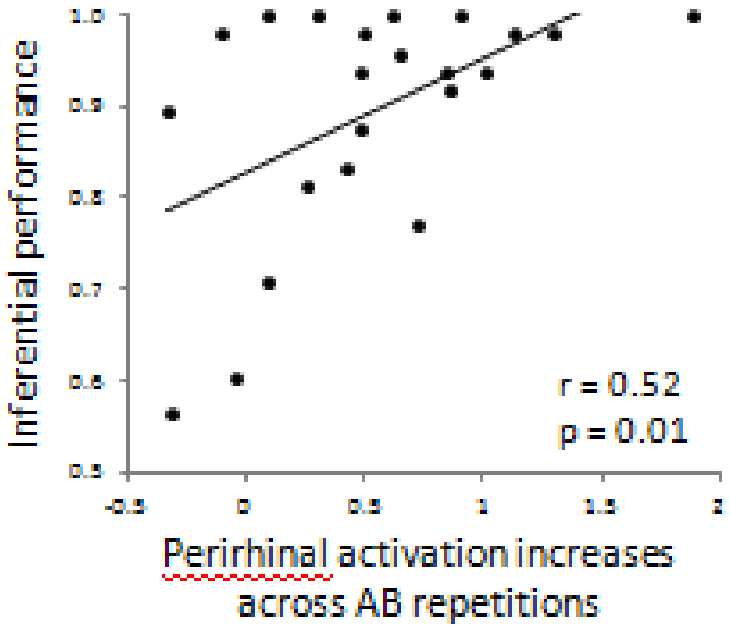

Figure 4. Activation increases across AB repetitions in bilateral perirhinal cortex track subsequent inferential (AC) performance.

References

[1] "Alzheimer's Disease Fact Sheet." *National Institute on Aging*. US Department of Health and Public Services. http://www.nia.nih.gov/alzheimers/publication/alzheimers-disease-fact-sheet

[2] "Parkinson's Disease Research Web Overview." *National Institute of Neurological Disorders and Stroke*. National Institute of Neurological Disorders and Stroke. http://www.ninds.nih.gov/research/parkinsonsweb/index.htm

[3] Visser PJ et al (2002). Medial temporal lobe atrophy predicts Alzheimer's disease in patients with minor cognitive impairment. J Neurol Neurosurg Psychiatry. 72:491–497

[4] Bertrand E et al (2003). Degenerative axonal changes in the hippocampus and amygdala in Parkinson's disease. Folia Neuropathol. 41(4):197-207.

[5] Squire LR et al (2004). The medial temporal lobe. Annu Rev Neurosci. 27:279-306

[6] Preston AR and Wagner AD (2007). The medial temporal lobe and memory in *Neurobiology of Learning and Memory, Second Edition*. Kesner RP and Martinez JL, Editors. Elseiver: Oxford. 305-337.

[7] Pihlajamaki, M., et al. Visual presentation of novel objects and new spatial arrangements of objects differentially activates the medial temporal lobe subareas in humans. Eur. J. Neurosci 2004. **19**: 1939–1949

[8] Suzuki, W.A. and Amaral, D.G.. Topographic organization of the reciprocal connections between monkey entorhinal cortex and the perirhinal and parahippocampal cortices. J. Neurosci, 1994. **14**: 1856-1877.

[9] O'Reilly, R.C. and J.W. Rudy, *Conjunctive representations in learning and memory: principles of cortical and hippocampal function.* Psychol Rev, 2001. **108**(2): p. 311-45.

[10] Kumaran, D. and E.A. Maguire, *Which computational mechanisms operate in the hippocampus during novelty detection?* Hippocampus, 2007. **17**(9): p. 735-48.

[11] Kumaran D, Maguire EA. Novelty signals: a window into hippocampal information processing.*Trending in Cognitive Sciences.* 2009;13:47–54.

[12] Hasselmo, M.E. and E. Schnell, *Laminar selectivity of the cholinergic suppression of synaptic transmission in rat hippocampal region CA1: computational modeling and brain slice physiology.* J Neurosci, 1994. **14**(6): p. 3898-914.

[13] Manns, J.R. and H. Eichenbaum, *Evolution of declarative memory.* Hippocampus, 2006. **16**(9): p. 795-808.

[14] Shohamy, D. and A.D. Wagner, *Integrating memories in the human brain: hippocampal-midbrain encoding of overlapping events.* Neuron, 2008. **60**(2): p. 378-89.

[15] Lisman J.E. and Grace A.A., The hippocampal-VTA loop: controlling the entry of information into long-term memory. Neuron, 2005. **46**: 703-713.

[16] Small, S.A., Nava, A.S., Perera, G.M., Delapaz, R., and Stern, Y., .Evaluating the function of hippocampal subregions with high-resolution MRI in Alzheimer's disease and aging. Microsc. Res. Tech., 2000. **51:** 101–108

[17] Duvernoy, H.. *The human hippocampus: Functional anatomy, vascularization and serial sections with MRI*, Third Edition (New York (2005): Springer).

[18] Carr V.A. et al., *Imaging the human medial temporal lobe with high-resolution fMRI.* Neuron. 2010 Feb 11;65(3):298-308.

[19] Zeithamova, D., & Preston, A.R. (2010). Flexible memories: Differential roles for medial temporal lobe and prefrontal cortex in cross-episode binding. Journal of Neuroscience, 30(44), 14676-14684.

[20] ANTS (http://www.picsl.upenn.edu/ANTS/, developed by the Penn Image Computing Science Lab).

[21] Chen, J., Olsen, R.K., Preston, A.R., Glover, G.H., & Wagner, A.D. (2011). Associative retrieval processes in the human medial temporal lobe: Hippocampal retrieval success and CA1 mismatch detection. Learning & Memory, 18(8), 523-528.